J M M
Journal of Mechanics and MEMS

ISSN: 0974-8407

9(2) 2017: pp. 253-263

Special Issue dedicated to Prof. K Y Ye edited by Z M Ye, P Liu and B Sun

QUASI-STATIC AND DYNAMIC BEHAVIOR OF INCOMPRESSIBLE SATURATED POROELASTIC ONE-DIMENSIONAL COLUMN ON LOCAL THERMAL NON-EQUILIBRIUM

Lu-wu He[1] and Xiao Yang[2]

ABSTRACT

Based on the thermo-hydro-mechanical coupled model for incompressible saturated porous media on local thermal non-equilibrium, the general analytic solutions of quasi-static and dynamic responses for incompressible saturated poroelastic one-dimensional column with adiabatic, fixed and impermeable at one end, subjected to mechanical and thermal loads and free permeation at the other end, are presented. Then, according to the general formulae, the quasi-static and dynamic responses of poroelastic column under a periodic thermal load are numerically studied. The variations and steady state amplitude ratios of the temperatures, solid displacements and effective stresses under local thermal non-equilibrium and equilibrium conditions with different parameters are discussed. The results show that, the differences between the temperatures obtained on local thermal non-equilibrium and equilibrium conditions exist in whole evolution and are dependent on the ratio of solid to fluid thermal diffusion coefficients, the heat exchange coefficient between solid and fluid and the frequency of the periodic thermal load. Those obvious differences induce that the solid displacements and effective stresses obtained on local thermal non-equilibrium and equilibrium conditions have evident changes, which also rely on the ratio of thermal consolidation to thermal diffusion coefficients.

***Keywords*:** Incompressible saturated poroelastic column, Local thermal non-equilibrium, Analytic solution, Quasi-static and dynamic and responses.

1. INTRODUCTION

Thermo-hydro-mechanical coupled response in a saturated deformable porous medium is important in many branches of engineering. Application can be found in diverse areas such as geothermal energy extraction, petroleum engineering, chemical engineering, agricultural engineering, geotechnical engineering, hazardous waste management and biomechanics. And this topic has also generated considerable attention in the field of high-level nuclear waste disposal in recent years. Based on Biot theory, Kurashige[1], Bai[2] and Zhou[3-4] established the coupled thermo-poroelastic models respectively, and numerically analyzed the thermal consolidation problems for saturated poroelastic one-dimensional column, and cylindrical and spherical cavitys under thermal loading. Bai Bing[5] discussed the physical meanings of every coupling term and their effects for the coupled thermo-poroelastic model[2], and numerically studied the thermal consolidation for layered, half-space saturated porous media subjected to exponential decaying thermal loading[6]. In addition, the numerical algorithm and its application for coupled thermal–hydraulic–chemical–mechanical model based on the hybrid mixture theory have been researched by several authors in detail, see Schrefler[7] and Seetharam[8]. All those models are founded on the local thermal equilibrium condition, that is, assuming the temperature of each phase is equal and using only one equation of conservation of energy to describe the phenomenon of heat transmission. However, the situation of local thermal non-equilibrium (each phase has different temperature) is more actual and ubiquitous. For example, if the velocity of fluid phase is high in porous

1. Key Lab of Safety Science of Pressurized System, Ministry of Education School of Mechanical and Power Engineering, East China University of Science and Technology, Shanghai, 200237, P. R. China

2. Department of Civil Engineering, Shanghai University, Shanghai 200444, P. R. China

medium or there is a continuous variable thermal load, it cannot guarantee that the temperatures of solid and fluid phases are equal. So the credible model of local thermal non-equilibrium should be established by applying two equations of conservation of energy. Up to now, the heat and mass transfer problems under the condition of local thermal non-equilibrium have plenty of researches[9-12], while the thermo-hydro-mechanical coupling analysis of porous media on local thermal non-equilibrium are few[13-14]. Based on the porous media theory (mixture theory with volume fractions) [15], Yang Xiao[16] established a fully coupling mathematical model for incompressible fluid-saturated porous medium on local thermal non-equilibrium, and also presented several Gurtin-type variational principles respectively. According to this coupled model and Gurtin-type variational principles, Qiu Wei-dong[17] developed a finite element numerical calculation procedure for general plane problems on local thermal non-equilibrium .

The purposes of the present study, according to the coupled model on local thermal non-equilibrium condition[16], are to develop a general analytic solution of quasi-static and dynamic responses for incompressible saturated poroelastic one-dimensional column with adiabatic, fixed and impermeable at one end, subjected to mechanical and thermal loads and free permeation at the other end. Those analytic solutions can provide a judgment criterion to verify the validity and precision of numerical methods. Finally, for the quasi-static and dynamic problem of poroelastic column under a periodic thermal load, the steady state amplitude ratios of the temperatures, solid displacements and effective stresses on local thermal non-equilibrium and equilibrium conditions with different parameters are studied. The differences between the temperatures, solid displacements and effective stresses obtained on local thermal non-equilibrium and equilibrium conditions are discussed.

2. BASIC EQUATIONS

Now consider a fluid saturated poroelastic column with finite length, as shown in Figure 1. Assume that it be permeable and subjected to combined mechanical and thermal loadings on its top end, and impermeable, heat insulation and displacement fixed at its bottom end. Neglecting bulk gravity, the governing equations for incompressible saturated poroelastic column on local thermal non-equilibrium can be written as follows[16]

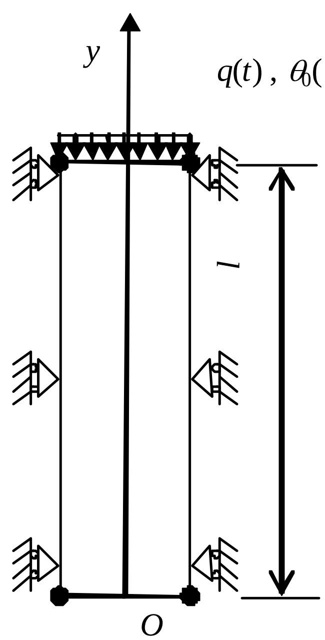

Figure 1: Fluid Saturated Poroelastic Column

$$
\begin{aligned}
&(\bar{\lambda}^S+2\bar{\mu}^S)\partial^2 u/\partial y^2-\partial p/\partial y-3\bar{K}^S\bar{\alpha}^S\partial\theta^S/\partial y-\bar{\rho}\,\partial^2 u/\partial t^2-\bar{\rho}^F\partial w/\partial t=0\\
&n^F\partial p/\partial y+\bar{S}_v w+\bar{\beta}_S\partial\theta^S/\partial y+\bar{\beta}_F\partial\theta^F/\partial y+\bar{\rho}^F(\partial^2 u/\partial t^2+\partial w/\partial t)=0\\
&\partial^2 u/\partial y\partial t+n^F\partial w/\partial y=0\\
&(\,t>0\,,\,0<y<l\,)
\end{aligned}
\qquad (1)
$$

and the boundary conditions can be expressed as

$$u(y,t)\big|_{y=0}=0\,,\;\; T_y(y,t)\big|_{y=l}=-q(t) \tag{2}$$

$$w(y,t)\big|_{y=0}=0, \quad p(y,t)\big|_{y=l}=0 \tag{3}$$

In addition, assume that there be not heat source in the poroelastic column and the influences of fluid velocity and solid deformation on temperature field are ignored, the governing equations for temperature field on local thermal non-equilibrium can be written as[16]

$$\begin{array}{l}\bar{\rho}_c^S\,\partial\theta^S/\partial t-(\bar{k}^{SS}\partial^2\theta^S/\partial y^2+\bar{k}^{SF}\partial^2\theta^F/\partial y^2)-\bar{e}_\theta(\theta^F-\theta^S)=0\\ \bar{\rho}_c^F\,\partial\theta^F/\partial t-(\bar{k}^{SF}\partial^2\theta^S/\partial y^2+\bar{k}^{FF}\partial^2\theta^F/\partial y^2)+\bar{e}_\theta(\theta^F-\theta^S)=0\end{array}\quad (t>0,\;0<y<l) \tag{4}$$

and the boundary conditions are

$$\partial\theta^S(y,t)/\partial y\big|_{y=0}=0\,,\;\;\theta^S(y,t)\big|_{y=l}=\theta_0(t)\,;\;\;\partial\theta^F(y,t)/\partial y\big|_{y=0}=0\,,\;\theta^F(y,t)\big|_{y=l}=\theta_0(t) \tag{5}$$

Without loss of generality, the initial conditions are taken as:

$$u(y,t)\big|_{t=0}=0\,,\;\;\partial u(y,t)/\partial t\big|_{t=0}=0\,,w(y,t)\big|_{t=0}=0 \tag{6}$$

$$\theta^S(y,t)\big|_{t=0}=0\,,\quad \theta^F(y,t)\big|_{t=0}=0 \tag{7}$$

In the above equations (1)-(7), all variables and parameters are dimensionless, and their definitions and physical meanings can be found in literatures [16-17] in detail. Here, t is time factor; n^F is the porosity; $u(y\,,t)$ and $w(y,t)$are the dimensionless solid displacement and fluid relative velocity, respectively; $\theta^S(y,t)$ and $\theta^F(y,t)$ are the dimensionless solid and fluid temperature, respectively; $p(y,t)$ is the dimensionless pore fluid pressure; $T_y(y,t)$ is the dimensionless total stress in y direction, and $T_y(y,t)=\sigma^{SE}{}_y(y,t)$- $p(y,t)$, $\sigma^{SE}{}_y(y,t)$ is the dimensionless solid effective stress in y direction.

3. SOLUTIONS OF TEMPERATURE FIELD

For the local thermal equilibrium condition, that is $\theta^S(y,t)\equiv\theta^F(y,t)$, setting $\theta(y,t)=\theta^S(\mathrm{y},\mathrm{t})\equiv\theta^F(y,t)$, equations (4), (5) and (7) are reduced to

$$\partial\theta/\partial t=a^2\partial^2\theta/\partial t^2 \quad (t>0, 0<y<l) \tag{8}$$

$$\partial\theta(y,t)/\partial t\big|_{y=0}=0\,,\theta(y,t)\big|_{y=l}=\theta_0(t);\;\theta(y,t)\big|_{t=0}=0 \tag{9}$$

where, $a^2=\bar{k}/\bar{\rho}_c$, $\bar{k}=\bar{k}^{SS}+2\bar{k}^{SF}+\bar{k}^{FF}$, $\bar{\rho}_c=\bar{\rho}_c^S+\bar{\rho}_c^F$. By using the separation variable method, the solution of initial-boundary value problem (8) and (9) can be obtained as follows

$$\theta(y,t)=\theta_0(t)+\sum_{n=0}^{\infty}T_\theta^{(n)}(t)\cos\lambda_n y,\,T_\theta^{(n)}(t)=-B_n e^{-(a\lambda_n)^2 t}\left(\int_0^t(\partial\theta_0(\tau)/\partial\tau)e^{(a\lambda_n)^2\tau}d\tau+\theta_0(0)\right) \tag{10}$$

where, $B_n=4(-1)^n/(1+2n)\pi$, $\lambda_n=(1+2n)\pi/2l$ $\quad(n=0, 1, 2, \ldots\ldots, \infty)$.

For the local thermal non-equilibrium condition, assume that the general solutions of temperature field are

$$\theta^S(y,t)=\theta_0(t)+\sum_{n=0}^{\infty}T_S^{(n)}(t)\cos\lambda_n y\,,\quad \theta^F(y,t)=\theta_0(t)+\sum_{n=0}^{\infty}T_F^{(n)}(t)\cos\lambda_n y \tag{11}$$

Obvious, equations (11) satisfy the boundary conditions (5) automatically. Substituting equations (11) into equations (4) and (7) results in

$$\begin{array}{l}\bar{\rho}_c^S\,\partial T_S^{(n)}/\partial t+(\bar{k}^{SS}\lambda_n^2T_S^{(n)}+\bar{k}^{SF}\lambda_n^2T_F^{(n)})-\bar{e}_\theta(T_F^{(n)}-T_S^{(n)})+\bar{\rho}_c^S\,B_n\partial\theta_0(t)/\partial t=0\\ \bar{\rho}_c^F\,\partial T_F^{(n)}/\partial t+(\bar{k}^{SF}\lambda_n^2T_S^{(n)}+\bar{k}^{FF}\lambda_n^2T_F^{(n)})+\bar{e}_\theta(T_F^{(n)}-T_S^{(n)})+\bar{\rho}_c^F\,B_n\partial\theta_0(t)/\partial t=0\end{array}\quad (\mathrm{t}>0) \tag{12}$$

$$T_S^{(n)}(t)\Big|_{t=0}=-B_n\theta_0(0)\,,T_F^{(n)}(t)\Big|_{t=0}=-B_n\theta_0(0) \tag{13}$$

Application of Laplace transform to equations (12) with the initial conditions (13), the solutions of initial value problem (12) and (13) are given as

$$\begin{aligned}
T_S^{(n)}(t)&=-I_n e^{s_1^{(n)}t}\left\{B_n\left(\int_0^t(\partial\theta_0(\tau)/\partial\tau)e^{-s_1^{(n)}\tau}d\tau+\theta_0(0)\right)\right\}-J_n e^{s_2^{(n)}t}\left\{B_n\left(\int_0^t(\partial\theta_0(\tau)/\partial\tau)e^{-s_2^{(n)}\tau}d\tau+\theta_0(0)\right)\right\}\\
T_F^{(n)}(t)&=-M_n e^{s_1^{(n)}t}\left\{B_n\left(\int_0^t(\partial\theta_0(\tau)/\partial\tau)e^{-s_1^{(n)}\tau}d\tau+\theta_0(0)\right)\right\}-N_n e^{s_2^{(n)}t}\left\{B_n\left(\int_0^t(\partial\theta_0(\tau)/\partial\tau)e^{-s_2^{(n)}\tau}d\tau+\theta_0(0)\right)\right\}
\end{aligned} \tag{14}$$

where

$$\begin{aligned}
&\alpha=\bar{k}^{FF}/\bar{k}^{SS},\beta=\bar{k}^{SF}/\bar{k}^{SS},\gamma=\bar{\rho}_c^F/\bar{\rho}_c^S\\
&a_S^2=\bar{k}^{SS}/\bar{\rho}_c^S=a^2(1+\gamma)/(1+\alpha+2\beta),\bar{e}_\theta^S=\bar{e}_\theta/\bar{\rho}_c^S=a^2e_h
\end{aligned} \tag{15}$$

$$\begin{aligned}
C_n&=a^2(1+1/\gamma)\left\{\frac{(\alpha-\gamma\beta)\lambda_n^2}{(1+2\beta+\alpha)}+e_h\right\},D_n=a^2(1+1/\gamma)\left\{\frac{(\gamma-\beta)\lambda_n^2}{(1+2\beta+\alpha)}+e_h\right\}\\
E_n&=a^2(1+1/\gamma)\left\{\frac{(\alpha+1)\lambda_n^2}{(1+2\beta+\alpha)}+e_h\right\},F_n=a^2(1+1/\gamma)\left\{\frac{(\alpha-\beta^2)(1+\gamma)\lambda_n^2}{(1+2\beta+\alpha)^2}+e_h\right\}
\end{aligned} \tag{16}$$

$$\begin{aligned}
&s_1^{(n)}=(-E_n+\sqrt{E_n^2-4F_n})/2<0\,,s_2^{(n)}=-(E_n+\sqrt{E_n^2-4F_n})/2<0\\
&I_n=(s_1^{(n)}+C_n)/(s_1^{(n)}-s_2^{(n)})\,,J_n=(s_2^{(n)}+C_n)/(s_2^{(n)}-s_1^{(n)})\\
&M_n=(s_1^{(n)}+D_n)/(s_1^{(n)}-s_2^{(n)})\,,N_n=(s_2^{(n)}+D_n)/(s_2^{(n)}-s_1^{(n)})
\end{aligned} \tag{17}$$

4. SOLUTIONS OF SOLID DISPLACEMENT AND EFFECTIVE STRESS

Substituting the second and third equations of (1) into the first equation of (1), the first equation of (1) can be changed into

$$\begin{aligned}
&(\bar{\lambda}^S+2\bar{\mu}^S)\partial^3u/\partial y^3-(\bar{\rho}+\bar{\rho}^F/(n^F)^2-2\bar{\rho}^F/n^F)\partial^3u/\partial y\partial t^2-[\bar{S}_v/(n^F)^2]\partial^2u/\partial y\partial t+\\
&+(\bar{\beta}_S/n^F-3\bar{K}^S\bar{\alpha}^S)\partial^2\theta^S/\partial y^2+(\bar{\beta}_F/n^F)\partial^2\theta^F/\partial y^2=0
\end{aligned} \tag{18}$$

With the aid of the stress-strain relationship $\sigma_y^{SE}=(2\bar{\mu}^S+\bar{\lambda}^S)\partial u/\partial y-3\bar{K}^S\bar{\alpha}^S\theta^S$ and the boundary condition (2), the boundary condition of $u(y, t)$ at $y = l$ can be expressed as

$$(\partial u/\partial y)\Big|_{y=l}=q_0(t)\equiv[(3\bar{K}^S\bar{\alpha}^S\theta^S-q(t))/(2\bar{\mu}^S+\bar{\lambda}^S)]\Big|_{y=l} \tag{19}$$

Suppose that the general solution of solid displacement be

$$u(y,t)=q_0(t)y+\sum_{n=0}^{\infty}T_u^{(n)}(t)\sin\lambda_n y \tag{20}$$

Obvious, equation (20) satisfies the boundary conditions (2) and (19) automatically. Substituting equation (20) into equations (18) and (6) results in

$$\begin{aligned}
&\partial^2T_u^{(n)}(t)/\partial t^2+2Q\partial T_u^{(n)}(t)/\partial t+2QA_nT_u^{(n)}(t)=f_n(t)\\
&T_u^{(n)}(t)\Big|_{t=0}=0,\partial T_u^{(n)}(t)/\partial t\Big|_{t=0}=R_n
\end{aligned} \tag{21}$$

where

$$
\begin{aligned}
&A_n = [\lambda_n^2 (n^F)^2 (\bar{\lambda}^S + 2\bar{\mu}^S)] / \bar{S}_v\,, \quad Q = \bar{S}_v / 2[(n^F)^2 \bar{\rho} + \bar{\rho}^F - 2n^F \bar{\rho}^F] \\
&f_n(t) \equiv -(B_n/\lambda_n)\partial^2 q_0(t)/\partial t^2 + 2Q\,\tilde{f}_n(t)\,, \quad R_n = 2\times(-1)^n l/(\lambda_n l)^2 \left(\partial q_0(t)/\partial t\right)\big|_{t=0} \\
&\tilde{f}_n(t) \equiv -(B_n/\lambda_n)\partial q_0(t)/\partial t - [\lambda_n (n^F)^2/\bar{S}_v][(\bar{\beta}_S/n^F - 3\bar{K}^S\bar{\alpha}^S)T_S^{(n)}(t) + (\bar{\beta}_F/n^F)T_F^{(n)}(t)]
\end{aligned}
\tag{22}
$$

Now only consider the case: $Q^2 - 2QA_n < 0$, namely, the parameter Q is smaller (underdamping). Setting $\xi_n = \sqrt{2QA_n - Q^2} > 0$, the solution of initial value problem (21) is given as

$$
T_u^{(n)}(t) = \frac{R_n}{\xi_n} e^{-Qt} \sin \xi_n t + \frac{1}{\xi_n}\int_0^t \left\{ f_n(\tau) e^{-Q(t-\tau)} \sin \xi_n (t-\tau) \right\} d\tau \tag{23}
$$

With the stress-strain relationship $\sigma_y^{SE} = (2\bar{\mu}^S + \bar{\lambda}^S)\partial u/\partial y - 3\bar{K}^S\bar{\alpha}^S\theta^S$ and equations (11) and (19), the general solution of solid effective stress σ_y^{SE} can be expressed as

$$
\begin{aligned}
\sigma_y^{SE}(y,t) &= (2\bar{\mu}^S + \bar{\lambda}^S)\partial u/\partial y - 3\bar{K}^S\bar{\alpha}^S\theta^S \\
&= (2\bar{\mu}^S + \bar{\lambda}^S) q_0(t) - 3\bar{K}^S\bar{\alpha}^S\theta_0(t) + \sum_{n=0}^{\infty}\left\{(2\bar{\mu}^S + \bar{\lambda}^S)T_u^{(n)}(t)\lambda_n - 3\bar{K}^S\bar{\alpha}^S T_S^{(n)}(t)\right\}\cos\lambda_n y
\end{aligned}
\tag{24}
$$

Substituting equations (11) and (20) into the second and third equations of (1) with equations (3) and (6), the general solutions of fluid relative velocity $w(y, t)$ and pore fluid pressure $p(y, t)$ can be obtained respectively.

For the local thermal equilibrium condition, the general solutions of solid displacement and effective stress can be obtained by substituting $T_\theta^{(n)}$ into equations (22)-(24) instead of $T_S^{(n)}$ and $T_F^{(n)}$, respectively. For the quasi-static response, omitting the terms $\partial^2 u / \partial t^2$ and $\partial w/\partial t$ from the first and second equations of (1) and the terms $\partial u(y,t)/\partial t\big|_{t=0} = 0$ and $w(y,t)\big|_{t=0} = 0$ from equation (6), similarly the above deductive procedure, the general solutions of solid displacement and effective stress can be obtained respectively.

5. NUMERICAL RESULTS AND DISCUSSION

As an application of the above general solutions formulae, consider the quasi-static and dynamic problem of poroelastic column subjected to a cosine periodic thermal load at $y = l$, i.e. $\theta_0(t) = \bar{\theta}_0(1-\cos\omega t)$ and $q(t) \equiv 0$.

In this case, from equations (10) and (14), $T_\theta^{(n)}(t)$, $T_S^{(n)}(t)$ and $T_F^{(n)}(t)$ have the following forms

$$
\begin{aligned}
T_\theta^{(n)}(t) &= A_\theta^{(n)} e^{-(a\lambda_n)^2 t} + B_\theta^{(n)} \sin\omega t + C_\theta^{(n)} \cos\omega t \\
T_S^{(n)}(t) &= A_{S1}^{(n)} e^{s_1^{(n)} t} + A_{S2}^{(n)} e^{s_2^{(n)} t} + B_S^{(n)} \sin\omega t + C_S^{(n)} \cos\omega t \\
T_F^{(n)}(t) &= A_{F1}^{(n)} e^{s_1^{(n)} t} + A_{F2}^{(n)} e^{s_2^{(n)} t} + B_F^{(n)} \sin\omega t + C_F^{(n)} \cos\omega t
\end{aligned}
\tag{25}
$$

where

$$
\begin{aligned}
&A_\theta^{(n)} = -\frac{\bar{\theta}_0\omega^2 B_n}{\omega^2 + (a\lambda_n)^4}\,,\; B_\theta^{(n)} = -\frac{\bar{\theta}_0\omega B_n (a\lambda_n)^2}{\omega^2 + (a\lambda_n)^4}\,,\; C_\theta^{(n)} = \frac{\bar{\theta}_0\omega^2 B_n}{\omega^2 + (a\lambda_n)^4}\,,\; A_{S1}^{(n)} = -\frac{\bar{\theta}_0\omega^2 B_n I_n}{\omega^2 + (s_1^{(n)})^2}\,,\; A_{S2}^{(n)} = -\frac{\bar{\theta}_0\omega^2 B_n J_n}{\omega^2 + (s_2^{(n)})^2} \\
&B_S^{(n)} = \bar{\theta}_0\omega B_n\left(\frac{I_n s_1^{(n)}}{\omega^2 + (s_1^{(n)})^2} + \frac{J_n s_2^{(n)}}{\omega^2 + (s_2^{(n)})^2}\right),\; C_S^{(n)} = \bar{\theta}_0\omega^2 B_n\left(\frac{I_n}{\omega^2 + (s_1^{(n)})^2} + \frac{J_n}{\omega^2 + (s_2^{(n)})^2}\right),\; A_{F1}^{(n)} = -\frac{\bar{\theta}_0\omega^2 B_n M_n}{\omega^2 + (s_1^{(n)})^2} \\
&A_{F2}^{(n)} = -\frac{\bar{\theta}_0\omega^2 B_n N_n}{\omega^2 + (s_2^{(n)})^2}\,,\; B_F^{(n)} = \bar{\theta}_0\omega B_n\left(\frac{M_n s_1^{(n)}}{\omega^2 + (s_1^{(n)})^2} + \frac{N_n s_2^{(n)}}{\omega^2 + (s_2^{(n)})^2}\right),\; C_F^{(n)} = \bar{\theta}_0\omega^2 B_n\left(\frac{M_n}{\omega^2 + (s_1^{(n)})^2} + \frac{N_n}{\omega^2 + (s_2^{(n)})^2}\right)
\end{aligned}
\tag{26}
$$

Using equations (10) and (14), the solutions of temperature field for the local thermal equilibrium and non-equilibrium conditions can be simplified to

$$\left.\begin{array}{c}\theta(y,t)=\theta_1(y,t)+r_\theta(y)\sin(\omega t+\varphi_\theta(y))\\ \theta^S(y,t)=\theta_{S1}(y,t)+r_{\theta S}(y)\sin(\omega t+\varphi_S(y)) \quad , \quad \theta^F(y,t)=\theta_F(y,t)+r_{\theta F}(y)\sin(\omega t+\varphi_F(y))\end{array}\right\} \tag{27}$$

where, $\lim_{t\to\infty}\theta_1(y,t)=\lim_{t\to\infty}\theta_{S1}(y,t)=\lim_{t\to\infty}\theta_{F1}(y,t)=\overline{\theta}_0$.

Similarly, the solutions of solid displacement and effective stress for the local thermal equilibrium and non-equilibrium conditions can be written as

$$\begin{array}{l}u^{eq}_{(q)}(y,t)=u^{eq}_{(q)_1}(y,t)+r^{eq}_{(q)_u}(y)\sin(\omega t+\varphi^{eq}_{(q)_u}(y))\\ u^{eq}_{(d)}(y,t)=u^{eq}_{(d)_1}(y,t)+e^{-Qt}u^{eq}_{(d)_2}(y,t)+r^{eq}_{(d)_u}(y)\sin(\omega t+\varphi^{eq}_{(d)_u}(y))\\ u^{neq}_{(q)}(y,t)=u^{neq}_{(q)_1}(y,t)+r^{neq}_{(q)_u}(y)\sin(\omega t+\varphi^{neq}_{(q)_u}(y))\\ u^{neq}_{(d)}(y,t)=u^{neq}_{(d)_1}(y,t)+e^{-Qt}u^{neq}_{(d)_2}(y,t)+r^{neq}_{(d)_u}(y)\sin(\omega t+\varphi^{neq}_{(d)_u}(y))\end{array} \tag{28}$$

$$\begin{array}{l}\sigma^{eq}_{y(q)}(y,t)=\sigma^{eq}_{(q)_1}(y,t)+r^{eq}_{(q)_\sigma}(y)\sin(\omega t+\varphi^{eq}_{(q)_\sigma}(y))\\ \sigma^{eq}_{y(d)}(y,t)=\sigma^{eq}_{(d)_1}(y,t)+e^{-Qt}\sigma^{eq}_{(d)_2}(y,t)+r^{eq}_{(d)_\sigma}(y)\sin(\omega t+\varphi^{eq}_{(d)_\sigma}(y))\\ \sigma^{neq}_{y(q)}(y,t)=\sigma^{neq}_{(q)_1}(y,t)+r^{neq}_{(q)_\sigma}(y)\sin(\omega t+\varphi^{neq}_{(q)_\sigma}(y))\\ \sigma^{neq}_{y(d)}(y,t)=\sigma^{neq}_{(d)_1}(y,t)+e^{-Qt}\sigma^{neq}_{(d)_2}(y,t)+r^{neq}_{(d)_\sigma}(y)\sin(\omega t+\varphi^{neq}_{(d)_\sigma}(y))\end{array} \tag{29}$$

where, the subscripts q and d denote the quasi-static and dynamic responses, respectively; the superscripts eq and neq denote the responses on local thermal equilibrium and non-equilibrium conditions, respectively; $\lim_{t\to\infty}\sigma^{eq}_{(q)_1}(y,t)=\lim_{t\to\infty}\sigma^{eq}_{(d)_1}(y,t)=\lim_{t\to\infty}\sigma^{eq}_{(q)_1}(y,t)=\lim_{t\to\infty}\sigma^{eq}_{(d)_1}(y,t)=0$, $\lim_{t\to\infty}u^{eq}_{(q)_1}(y,t)=\lim_{t\to\infty}u^{eq}_{(d)_1}(y,t)=\lim_{t\to\infty}u^{neq}_{(q)_1}(y,t)=\lim_{t\to\infty}u^{neq}_{(d)_1}(y,t)$ $=q_0(t)y; u^{eq}_{(d)_2}(y,t)$, $u^{neq}_{(d)_2}(y,t)$, $\sigma^{eq}_{(d)_2}(y,t)$ and $\sigma^{neq}_{(d)_2}(y,t)$ are limited functions, respectively.

From expressions (27), it is found that the solutions of temperature field for the local thermal equilibrium and non-equilibrium conditions include two parts: transient and steady sate responses. All steady sate period are equal to the period of thermal load, but their steady state amplitudes and phase angles are different each other. From expressions (28) and (29), it is found that the solid displacement and effective stress have the same behaviors with the solutions of temperature field. The only difference in dynamic response is that there exists a transient sate response related to the inertial effect.

Due to many parameters involved in the quasi-static and dynamic analysis, specially takes[5,17] : $n^F=0.4, \overline{\lambda}^S=0.6, \overline{\mu}^S=0.4, \overline{K}^S=0.867$, $\overline{\rho}=3.4\times10^{-3}, \overline{\rho}^F=0.7\times10^{-3}, \overline{\alpha}^S=8.9\times10^{-5}, \gamma=1.346$, $l=10$, $\overline{\theta}_0=25$ and β = 0.005 in the following numerical calculation. In addition, to examine the thermal diffusion influence in the thermal consolidation, introduces a dimensionless parameter $c/\kappa=(n^F)^2\overline{\rho}_c/\overline{S}_v\overline{k}=(n^F)^2/\overline{S}_v a^2$, in which c and κ are the thermal consolidation coefficient and the thermal diffusion coefficient, respectively.

Because equations (1) and (4) are linear, the steady state amplitude ratios of the temperatures, the solid displacement and effective stress on between local thermal equilibrium and non-equilibrium conditions are independent of $\overline{\theta}_0$. Under the situation of some parameters given above, the steady state amplitude ratios $r_{\theta s}(y)$ / $r_\theta(y)$ and $r_{\theta F}(y)$ / $r_\theta(y)$ are only dependent on parameters α, $\overline{e}^S_\theta/a^2$ and ω/a^2; the steady state amplitude ratios $r^{neq}_{(q)_u}(y)/r^{eq}_{(q)_u}(y)$ and $r^{neq}_{(q)_\sigma}(y)/r^{eq}_{(q)_\sigma}(y)$ are dependent on parameters α, $\overline{e}^S_\theta/a^2$, ω/a^2, $\overline{\beta}_S$, $\overline{\beta}_F$ and c/κ. Therefore, the real value of a is not important to the analysis of temperatures and quasi-static response. The steady state amplitude ratios $r^{neq}_{(d)\ u}(y)/r^{eq}_{(d)_u}(y)$ and $r^{neq}_{(d)\ \sigma}(y)/r^{eq}_{(d)_\sigma}(y)$ are also dependent on parameter Q by contrast with $r^{neq}_{(q)\ u}(y)/r^{eq}_{(q)_u}(y)$ and $r^{neq}_{(q)\ \sigma}(y)/r^{eq}_{(q)_\sigma}(y)$.

Table 1(a = 1) presents the steady state amplitude ratios $r_{\theta S}(0)$ / $r_\theta(0)$ and $r_{\theta F}(0)/r_\theta(0)$ with different parameters α, $\bar{e}^S_\theta/a^2$ and ω/a^2. It shows that $r_{\theta S}(0)$ / $r_\theta(0) > 1$ (<1) and $r_{\theta F}(0)/r_\theta(0) < 1$ (>1) when $\alpha/\gamma > 1$ (<1), i.e. the thermal diffusion coefficient of fluid phase is larger (smaller) than that of solid phase. Further numerical results show that $r_{\theta S}(0)$ / $r_\theta(0)$ and $r_{\theta F}(0)/r_\theta(0)$ are close to one as $\bar{e}^S_\theta/a^2$ is increases; the smaller ω/a^2 is, the more obvious trends of $r_\theta(0)$, $r_{\theta S}(0)$ and $r_{\theta F}(0)$ close to $\bar{\theta}_0$ are. For relatively larger $\omega/a^2 \geq 1$, though the variations of $r_{\theta S}(0)$ / $r_\theta(0)$ and $r_{\theta F}(0)$ / $r_\theta(0)$ with parameter α/γ are complicated, $r_\theta(0)/\bar{\theta}_0$, $r_{\theta S}(0)/\bar{\theta}_0$ and $r_{\theta F}(0)/\bar{\theta}_0$ are approximate to zero.

For $\omega/a^2 = 0.05$, $\bar{e}^S_\theta/a^2 = 10^{-3}$ and $\bar{\beta}_S = \bar{\beta}_F = 1.0\times10^{-4}\bar{S}_v$, Table 2 presents the steady state amplitude ratios $r^{neq}_{(q)\ u}(l)/r^{eq}_{(q)_u}(l), r^{neq}_{(d)\ u}(l)/r^{eq}_{(d)_u}(l), r^{neq}_{(q)\ \sigma}(0)/r^{eq}_{(q)_\sigma}(0)$ and $r^{neq}_{(d)\ \sigma}(0)/r^{eq}_{(d)_\sigma}(0)$ with different parameters α and c/κ. Considering the confined condition $Q^2 - 2QA_n < 0$, specially take a = 10 in Table 2, and the parameters $\bar{S}_v$ and Q are determined by the given parameter c/κ. Table 3 (a = 1) presents the steady state amplitude ratios $r^{neq}_{(q)\ u}(l)/r^{eq}_{(q)_u}(l)$, $r^{neq}_{(d)\ u}(l)/r^{eq}_{(d)_u}(l)$, $r^{neq}_{(q)\ \sigma}(0)/r^{eq}_{(q)_\sigma}(0)$ and $r^{neq}_{(d)\ \sigma}(0)/r^{eq}_{(d)_\sigma}(0)$ with different parameters α and c/κ. In Tables 2 and 3, some $T^{(n)}_u(t)$ in equation (21) are overdamping when $c/\kappa \leq 40/a^2$. From Table 2, it is found that the variation of $r^{neq}_{(q)\ u}(l)/r^{eq}_{(q)_u}(l)$, $r^{neq}_{(q)\ \sigma}(0)/r^{eq}_{(q)_\sigma}(0)$ and $r^{neq}_{(d)\ \sigma}(0)/r^{eq}_{(d)_\sigma}(0)$ with parameters α is very similar to that of $r_{\theta S}(0)/r_\theta(0)$ and $r_{\theta F}(0)/r_\theta(0)$, but the variation of $r^{neq}_{(d)\ u}(l)/r^{eq}_{(d)_u}(l)$ ($c/\kappa \leq 2.0$) with parameters α is opposite to that of $r_{\theta S}(0)/r_\theta(0)$ and $r_{\theta F}(0)/r_\theta(0)$; with the parameter c/κ increasing, all go to their limit values, respectively; $r^{neq}_{(q)\ u}(l)/r^{eq}_{(q)_u}(l)$ and $r^{neq}_{(q)\ \sigma}(0)/r^{eq}_{(q)_\sigma}(0)$ compared with $r^{neq}_{(d)\ u}(l)/r^{eq}_{(d)_u}(l)$ and $r^{neq}_{(d)\ \sigma}(0)/r^{eq}_{(d)_\sigma}(0)$ have obvious different. For the given parameter $c/_\kappa$, Q and $\bar{\beta}_S = \bar{\beta}_F$ in Table 3 is 100 times of that in Table 2, respectively. By contrast to the corresponding results in Tables 2 and 3, it is found that the influence of parameter $\bar{\beta}_S = \bar{\beta}_F$ for $r^{neq}_{(q)\ u}(l)/r^{eq}_{(q)_u}(l)$ and $r^{neq}_{(q)\ \sigma}(0)/r^{eq}_{(q)_\sigma}(0)$ is evident, but the influence of parameter $\bar{\beta}_S = \bar{\beta}_F$ for the limit value of $r^{neq}_{(q)\ u}(l)/r^{eq}_{(q)_u}(l)$ with c/κ increasing is feebler. From Table 3 (c/κ = 50,100), it is found that the difference between the quasi-static and dynamic responses is unobvious when the parameter Q is larger.

For $\alpha = 4.0$, $\omega/a^2 = 0.05$, $\bar{e}^S_\theta/a^2 = 10^{-3}$ and $\bar{\beta}_S = \bar{\beta}_F = 0$, Figure 2 and 3 ($a$ = 10) present the variation of solid effective stress with time factor t at (y = 0) for c/κ = 0.5, 3.0 in the quasi-static and dynamic responses, respectively. Figure 2 and 3 show that the solid effective stress at (y = 0) is firstly compressive stress at the beginning stage because of the heat expansion effect; the vibration amplitude of solid effective stress in the dynamic response at the beginning stage is far larger than that of solid effective stress in the quasi-static response; and when the parameter c/κ increases (namely, the parameters $\bar{S}_v$ and Q decrease and the permeability increases), the vibration amplitude of solid effective stress in the dynamic response increases, but the vibration amplitude of solid effective stress in the quasi-static response decreases. Figure 2 and 3 also show that the steady state amplitude of solid effective stress in the dynamic response is larger than that of solid effective stress in the quasi-static response; $r^{neq}_{(q)\ \sigma}(0)$, $r^{eq}_{(q)_\sigma}(0)$, $r^{neq}_{(d)\ \sigma}(0)$ and $r^{eq}_{(d)_\sigma}(0)$ are decreasing when the parameter c/κ is increasing. As $c/\kappa\to\infty$, $\left(r^{neq}_{(q)\ \sigma}(0), r^{eq}_{(q)_\sigma}(0), r^{neq}_{(d)\ \sigma}(0), r^{eq}_{(d)_\sigma}(0)\right)\to$ (0.0, 0.0, 3.294×10^{-3}, 5.586×10^{-3}). Further numerical results show that the solid displacement at (y = l) in the dynamic response still has the possibility of $u(t) \leq 0$ at the beginning stage in despite of $\theta_0(t) \geq 0$; the steady state amplitude of solid displacement in the dynamic response is smaller than that of solid displacement in the quasi-static response; and $r^{neq}_{(q)\,u}(l)$, $r^{eq}_{(q)_u}(l)$, $r^{neq}_{(d)\,u}(l)$ and $r^{eq}_{(d)_u}(l)$ are increasing when the parameter c/κ is increasing. As $c/\kappa \to \infty$, $\left(r^{neq}_{(q)\,u}(l), r^{eq}_{(q)_u}(l), r^{neq}_{(d)\,u}(l), r^{eq}_{(d)_u}(l)\right)\left(2\bar{\mu}^S + \bar{\lambda}^S\right) \to \left(3\bar{K}^S\bar{\alpha}^S\bar{\theta}_0 l\right)(0.313, 0.487, 0.198, 0.200)$.

6. CONCLUSIONS

Based on the thermo-hydro-mechanical coupled model for incompressible saturated porous media on local thermal non-equilibrium, the general analytic solutions of quasi-static and dynamic responses for incompressible saturated poroelastic one-dimensional column with adiabatic, fixed and impermeable at one end, subjected to mechanical and thermal loads and free permeation at the other end, are obtained. For cosine periodic thermal load, the quasi-static and dynamic responses of poroelastic column with different parameters are numerically studied. The study results show that

(1) the differences between the temperatures obtained on local thermal non-equilibrium and equilibrium conditions exist in whole evolution and the steady state amplitude ratios are dependent on the parameters α/γ (ratio of solid to fluid thermal diffusion coefficients), $\bar{e}^S_\theta / a^2$ (ratio of heat exchange coefficient between solid and fluid to thermal diffusion coefficient on local thermal equilibrium) and ω/a^2 (ratio of frequency of the periodic thermal load to thermal diffusion coefficient on local thermal equilibrium). As $\bar{e}^S_\theta / a^2$ is increasing, the steady state amplitude ratios are approximate to 1; the smaller (or larger) ω/a^2 is, the more unobvious the differences of steady state amplitudes on between local thermal non-equilibrium and equilibrium conditions are.

(2) the apparent differences between the temperatures obtained on local thermal non-equilibrium and equilibrium conditions induce that the solid displacements and effective stresses obtained on local thermal non-equilibrium and equilibrium conditions have obvious changes, which also rely on the parameter c/κ (ratio of thermal consolidation to thermal diffusion coefficients). The steady state amplitudes and ratios in quasi-static response compared with those in dynamic response are also different. At the beginning stage, as the parameter Q is decreasing, the vibration amplitude of solid displacement at top and effective stress at bottom in the dynamic response is increasing, and is far larger than that of solid displacement at top and effective stress at bottom in the quasi-static response. As the parameter c/κ is increasing, the steady state amplitudes of solid displacement at top is increasing and the steady state amplitudes of effective stress at bottom is decreasing, but they are all going to their limit values.

The study results also reveal that it is important to consider and distinguish the difference of between results obtained on local thermal non-equilibrium and equilibrium conditions in the thermal stress analysis for porous medium or structures.

Table 1
Steady State Amplitude Ratios of Temperatures on Local Thermal Non-equilibrium and Equilibrium

			α					
			0.1	*0.5*	*2.0*	*4.0*	*8.0*	*10*
$\frac{\omega}{a^2}=0.005$	$\bar{e}^S_\theta/a^2=10^{-3}$	$r_{\theta S}(0)/r_\theta(0)$	1.036	1.014	0.989	0.944	0.840	0.789
		$r_{\theta F}(0)/r_\theta(0)$	0.650	0.962	1.005	1.008	1.007	1.006
	$\bar{e}^S_\theta/a^2=10^{-2}$	$r_{\theta S}(0)/r_\theta(0)$	0.985	1.001	0.996	0.982	0.958	0.948
		$r_{\theta F}(0)/r_\theta(0)$	0.907	0.985	1.001	0.999	0.991	0.989
$\frac{\omega}{a^2}=0.05$	$\bar{e}^S_\theta/a^2=10^{-3}$	$r_{\theta S}(0)/r_\theta(0)$	1.668	1.407	0.809	0.481	0.227	0.165
		$r_{\theta F}(0)/r_\theta(0)$	0.029	0.584	1.126	1.288	1.381	1.401
	$\bar{e}^S_\theta/a^2=10^{-2}$	$r_{\theta S}(0)/r_\theta(0)$	1.466	1.271	0.874	0.647	0.441	0.384
		$r_{\theta F}(0)/r_\theta(0)$	0.257	0.709	1.082	1.185	1.246	1.260
$\frac{\omega}{a^2}=1.0$	$\bar{e}^S_\theta/a^2=10^{-3}$	$r_{\theta S}(0)/r_\theta(0)$	7.912	3.713	0.360	0.069	0.043	0.038
		$r_{\theta F}(0)/r_\theta(0)$	0.329	0.167	1.608	2.834	3.918	4.193
	$\bar{e}^S_\theta/a^2=10^{-2}$	$r_{\theta S}(0)/r_\theta(0)$	7.746	3.627	0.391	0.061	0.060	0.055
		$r_{\theta F}(0)/r_\theta(0)$	0.328	0.157	1.582	2.780	3.845	4.115

Table 2
Steady State Amplitude Ratios of Solid Displacements and Effective Stresses on Local Thermal Non-equilibrium and Equilibrium (a = 10)

		α					
		0.1	*0.5*	*2.0*	*4.0*	*8.0*	*10*
	c / κ = 0.5	1.441	1.224	0.937	0.878	0.813	0.778
$r_{u(q)}^{neq}(l)/r_{u(q)}^{eq}(l)$	c / κ = 2.0	1.603	1.347	0.853	0.638	0.500	0.463
	c / κ = 10	1.536	1.313	0.860	0.637	0.474	0.430
	c / κ = 100	1.518	1.304	0.863	0.641	0.476	0.432
$r_{\sigma(q)}^{neq}(0)/r_{\sigma(q)}^{eq}(0)$	c / κ = 0.5	1.564	1.338	0.839	0.555	0.324	0.265
	c / κ = 2.0	1.623	1.372	0.825	0.524	0.294	0.240
	c / κ = 10	1.644	1.385	0.820	0.513	0.284	0.231
	c / κ = 100	1.649	1.388	0.819	0.510	0.282	0.229
	c / κ = 0.5	0.926	0.874	1.091	1.218	1.183	1.132
$r_{u(d)}^{neq}(l)/r_{u(d)}^{eq}(l)$	c / κ = 2.0	0.640	0.761	1.107	1.237	1.203	1.153
	c / κ = 10	0.916	0.946	1.020	1.021	0.936	0.888
	c / κ = 100	0.950	0.969	1.008	0.990	0.896	0.848
	c / κ = 0.5	1.467	1.278	0.866	0.624	0.411	0.351
$r_{\sigma(d)}^{neq}(0)/r_{\sigma(d)}^{eq}(0)$	c / κ = 2.0	1.535	1.316	0.853	0.602	0.400	0.345
	c / κ = 10	1.563	1.332	0.848	0.593	0.395	0.343
	c / κ = 100	1.571	1.334	0.846	0.590	0.394	0.342

Table 3
Steady State Amplitude Ratios of Solid Displacements and Effective Stresses on Local Thermal Non-equilibrium and Equilibrium (a = 1)

		α					
		0.1	*0.5*	*2.0*	*4.0*	*8.0*	*10*
	c / κ = 0.5	1.184	1.082	0.974	0.943	0.912	0.898
	c / κ = 2.0	1.517	1.290	0.885	0.726	0.627	0.600
$r_{u(q)}^{neq}(l)/r_{u(q)}^{eq}(l)$	c / κ = 10	1.534	1.310	0.863	0.646	0.489	0.447
	c / κ = 50	1.520	1.304	0.863	0.642	0.478	0.434
	c / κ = 100	1.518	1.303	0.864	0.642	0.477	0.433
	c / κ = 0.5	2.521	1.743	0.696	0.280	0.355	0.412
	c / κ = 2.0	2.497	1.798	0.670	0.230	0.364	0.431
$r_{\sigma(q)}^{neq}(0)/r_{\sigma(q)}^{eq}(0)$	c / κ = 10	2.505	1.820	0.661	0.216	0.368	0.436
	c / κ = 50	2.507	1.825	0.660	0.213	0.369	0.437
	c / κ = 100	2.507	1.826	0.659	0.213	0.369	0.438
	c / κ = 50	1.520	1.304	0.863	0.642	0.478	0.434
$r_{u(d)}^{neq}(l)/r_{u(d)}^{eq}(l)$	c / κ = 100	1.518	1.304	0.864	0.642	0.477	0.433
	c / κ = 1000	1.516	1.303	0.864	0.642	0.476	0.432
	c / κ = 50	2.511	1.828	0.658	0.204	0.364	0.434
$r_{\sigma(d)}^{neq}(0)/r_{\sigma(d)}^{eq}(0)$	c / κ = 100	2.514	1.831	0.656	0.195	0.360	0.431
	c / κ = 1000	2.469	1.820	0.653	0.101	0.274	0.353

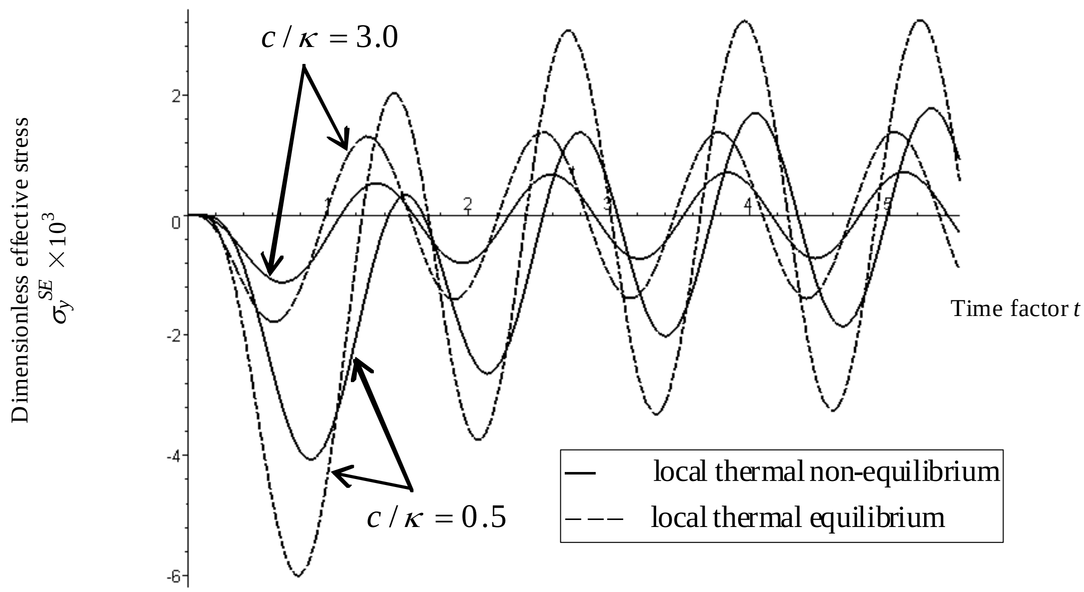

Figure 2: Dimensionless Solid Effective Stress of Poroelastic Column at y = 0 vs. Time Factor t (Quasi-static Response s)

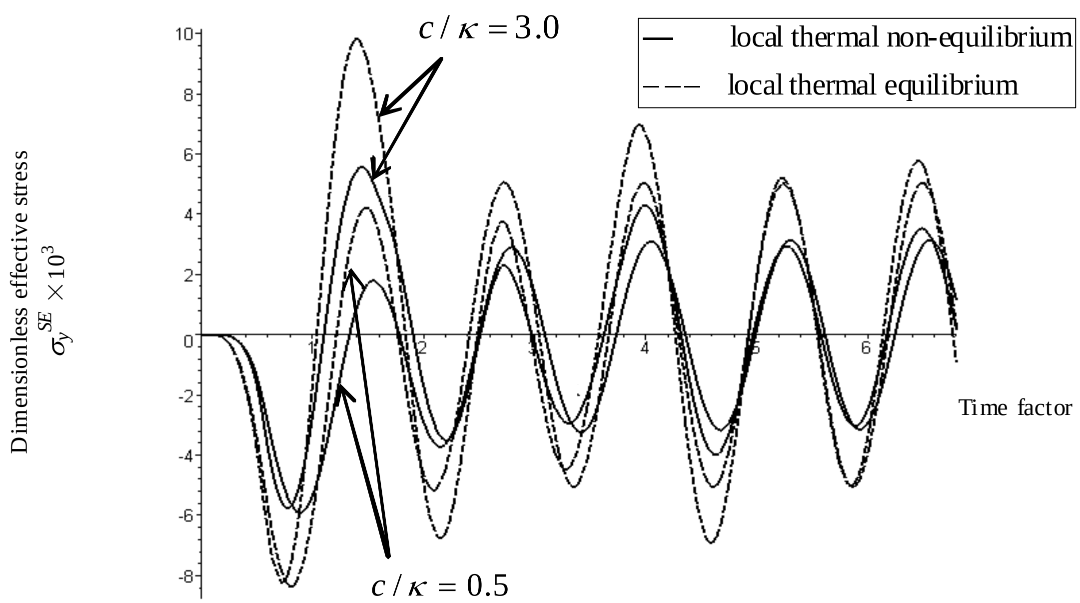

Figure 3: Dimensionless Solid Effective Stress of Poroelastic Column at y = 0 vs. Time Factor t (Dynamic Responses)

References

[1] Kurashjge M. A Thermoelastic Theory of Fluid-filled Porous Materials [J], *Int. J. Solids and Structures*, 1989, **25**(9): 1039-1052.

[2] Bai M., Abousleiman Y. Thermoporoelastic Coupling with Application to Consolidation [J], *Int. J. Numerical and Analytical Methods in Geomechanics*, 1997, 21: 121-132.

[3] Zhou Y., Rajapakse R. K. N. D., Graham J. A Coupled Thermoporoelastic Model with Thermo-osmosis and Thermai-filtration [J], *Int. J. Solids and Structures*, 1998, 35(34-35): 4659-4683.

[4] Zhou Y., Rajapakse R. K. N. D., Graham J. Coupled Consolidation of a Porous Medium with a Cylindrical or a Spherical Cavity [J], *Int. J. Numerical and Analytical Methods in Geomechanics*, 1998, 22: 449-475.

[5] Bai Bing. Effects of Coupling Schemes Thermo-hydro-mechanical Governing Equations for Saturated Porous Medium [J], *Rock and Soil Mechanics*, 2006, 27(4): 519-524. (in Chinese).

[6] Bai Bing, Thermal Consolidation of Layered Porous Half-space to Variable Thermal Loading [J], *Applied Mathematics and Mechanics (English Edition)*, 2006, 27(11): 1531-1539.

[7] Lewis R. W., Schrefler, B. A. The Finite Element Method in the Static and Dynamic Deformation and Consolidation of Porous Media [M], *Chichester, England: Wiley (Second Edition)*, 1998.

[8] Seetharam S. C., Thomas H. R., Cleall P. J., Coupled thermo/hydro/chemical/mechanical model for unsaturated soils—Numerical Algorithm [J], *Int. J. Numer. Meth. Engng.*, 2007, 70: 1480-1511.

[9] Nield D. A., Kuznetsov A. V., Thermally Developing Forced Convection in a Channel Occupied by a Porous Medium Saturated by a Non-Newtonian Fluid [J], *Int. J. Heat and Mass Transfer*, 2005, 48(6): 1214-1218.

[10] Yang Xiao, Liu Xue-mei. Temperature Profile of Local Thermal Nonequilibrium for Thermal Developing Forced Convection in a Porous Medium Parallel Plate Channel [J], *Applied Mathematics and Mechanics (English Edition)*, 2006, 27(8): 1123-1131.

[11] Nield D. A., Kuznetsov A. V., Natural Convection about a Vertical Plate Embedded in a Bidisperse Porous Medium [J], *Int. J. Heat and Mass Transfer*, 2007, 51(7): 1658-1664.

[12] Malashetty M. S., Mahantesh S., Rajashekhar H., Double Diffusive Convection in a Porous Layer using a Thermal Non-equilibrium Model [J], *Int. J. Thermal Sciences*, 2008, 47: 1131-1147.

[13] Gajo A. A Non-linear Analysis of Non-isothermal Wave Propagation in Linear-elastic Fluid-saturated Porous Media[J], *Int J. Plasticity*, 2002, 18(3): 313-344.

[14] Yang Xiao, Liu Xue-mei. Thermal Stress of Local Thermally Nonequilibrium for Forced Convection in a Porous Medium Parallel Plate Channel [J], *Acta Mechanica Solida Sinica*, 2006, 27(3): 293-297. (in Chinese).

[15] de Boer R. Reflections on the Development of the Theory of Porous Media [J]. *Applied Mechanics Review*, 2003, 56(6): 27-42.

[16] Yang Xiao, Gurtin-type Variational Principles for Dynamics of a Non-local Thermal Equilibrium Saturated Porous Medium [J], *Acta Mechanica Solida Sinica*, 2005, 18(1), 37-45.

[17] Qiu Wei-dong. The Dynamical Consolidation of Saturated Porous Media on Local Thermal Non-equilibrium [D], *Master Thesis of East China University of Science and Technology*, 2008. (in Chinese).